Finite element analysis of a novel building integrated solar thermal vacuum flat plate collector for water and space heating

Gaurav Nanajkar[1] and Prof. Philip Eames[1]

[1]CREST, Wolfson School of Electrical, Electronics and System Engineering
Loughborough University, United Kingdom

Abstract

A novel building integrated solar thermal vacuum flat plate collector can potentially provide heat to charge a compact thermal storage system at 150-200˚C. The purpose of the proposed design is to achieve higher operating temperatures efficiently which can increase the potential applications for heating and cooling. The design features facilitate easy integration in the building envelope. The high vacuum pressure inside the designed envelope leads to a pressure differential between the vacuum space and the ambient environment. A finite element analysis (FEA) was performed to assess the structural design safety, it was found from simulations that the stresses are within material safety limits. FEA predictions are compared with predictions using classical plate bending theory along with column buckling calculations. FEA results comparison with classical plate bending theory is followed by the experimental results using digital image correlation (DIC).

Keywords: Vacuum flat plate collector; solar thermal; compound parabolic concentrator, FEA, classical plate bending; column buckling; Digital image correlation (DIC)

1. Introduction

The Paris agreement (COP 21) that took place in 2015, may prove to be a historic milestone for the global energy sector, sending a strong signal through its aims to limit global greenhouse gas emissions as soon as possible to keep the global temperature increase well below 2°C. The building sector consumes nearly one-third of global final energy consumption, making it responsible for nearly one-third of total CO_2 emissions. Currently, space heating and cooling along with water heating are estimated to account for nearly 60% of total energy consumption in buildings. They therefore represent the single largest opportunity for reducing building energy consumption and associated CO_2 emission.

In order to address this opportunity a novel solar thermal collector was designed which can potentially supply heat at 150-200°C to charge a compact thermal energy storage unit, allowing heat to be stored for long term and thus meet a greater fraction of annual space heating and cooling and water heating. To enhance the efficiency of the solar collector at high temperatures suppression of heat losses are crucial. High vacuum pressure can be used to suppress the loses, however this exerts a pressure on the collector envelope due to the pressure difference between the atmosphere and the vacuum. A finite element analysis and experimental digital image correlation technique was used to examine the structural design safety required to and maintain the system integrity for a minimum 20-year lifetime with results presented in this paper**.**

2. Design Concept

A novel solar thermal flat plate collector design is proposed based on a combination of elements from traditional flat plate collectors, evacuated tubes and compound parabolic concentrating collectors. Design elements from a flat plate collector are coupled with vacuum technology from evacuated tube collectors and a non-imaging compound parabolic concentrator with an acceptance angle of 45˚ as shown in figure 1.

doi:10.18086/swc.2019.01.06 Available at http://proceedings.ises.org

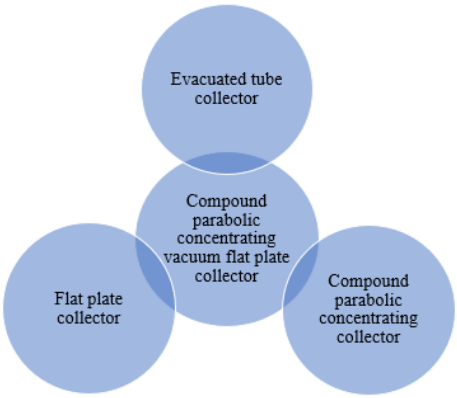

Figure 1. The design concept for the proposed novel solar thermal collector

As shown in figure 2, design consists of an evacuated envelope formed by a stainless-steel enclosure base section (back and side walls of the vacuum enclosure) with a glass cover sheet evacuated to a pressure less than 10^{-3} mbar to suppress gaseous conduction, convection losses and heat exchange will take place only through radiation. An array of low concentration compound parabolic concentrating (CPC) collector units is enclosed in the envelope. To support the glass cover and prevent fracture due to the pressure differential between the vacuum space and the ambient environment, the glazing is supported by slender columns running between the alternate CPC reflectors.

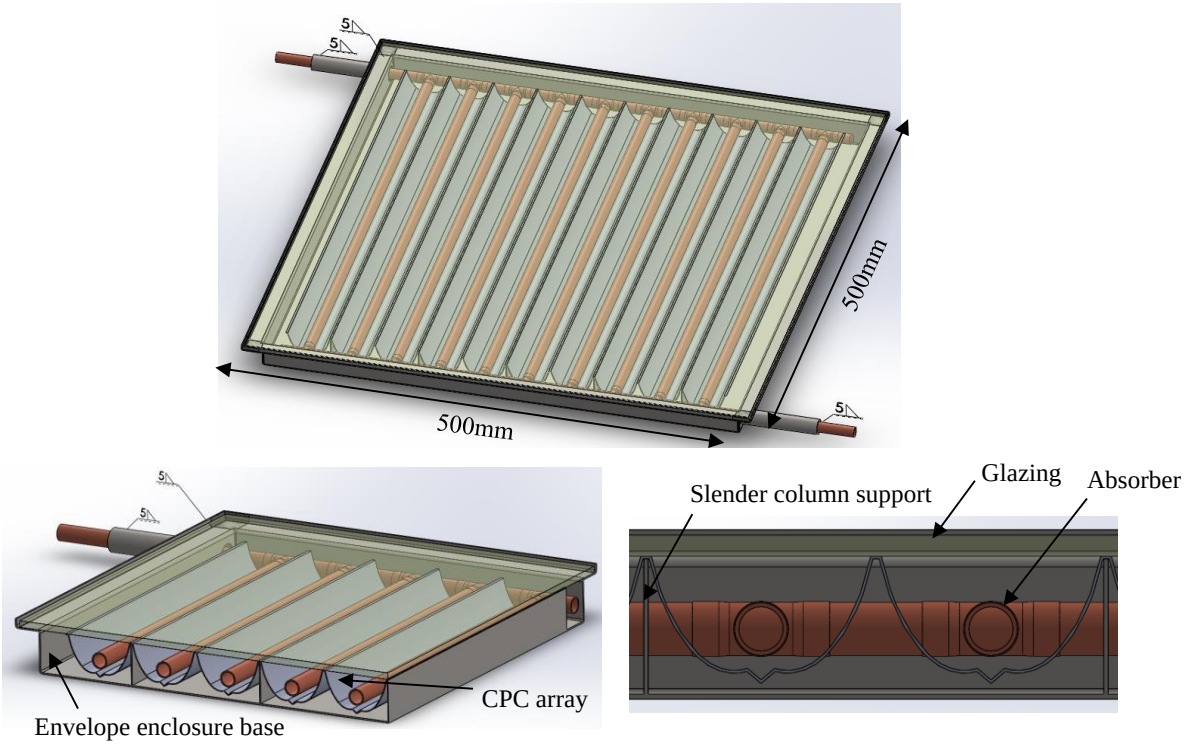

Figure 2. Schematic diagrams of the proposed novel compound parabolic concentrating vacuum flat plate collector

When the envelope is evacuated, the total load acting on the slender column will be the difference between the internal and external gas pressures. In the case of the horizontal or inclined position of the panel, the weight of glazing will be an additional load. By using a slender column, the active area exposed to the insolation can be maximised.

The novel collector design is slim and modular, making it easy to integrate into a building envelope. The use of a suitable non-evaporable getter within the envelope can potentially maintain the required vacuum pressure to suppress conductive and convective heat transfer for the required 15 to 20 years lifetime.

3. Literature Review

Arya, F. et al. (2016), designed a slim novel vacuum flat plate collector with the glass cover supported using an array of pillars, the vacuum pressure was less than 0.001 mbar to suppress gaseous conduction and convection. Henshall, P. et al. (2016), explored the mechanical stresses in a similar vacuum flat plate collector using an FEA model which was validated against experimental measurements from a prototype system. This paper suggested replacing the tempered glass on one side of the enclosure by a thin flexible metal sheet to minimize the stress generation caused due to the undulating surface created by the roller wave effect during tempering, however, research to assess the optimal thickness of the sheet was not undertaken.

The FEA model developed in the current research is based on the FEA model used for vacuum glazing by Wang, J. et al. (2007) and Simko, T. M. et al. (1998). They identified various design constraints including maximum permissible stress allowed on the external glass aperture cover surface, the maximum stress to guarantee that Hertzian indentation fracture did not occur on the inside glass surface and the maximum compressive stress on the support pillar which should be less than the compressive strength of the material used. Though the use of support pillars was safe under high vacuum, it formed a conductive path for heat transfer. Due to the considerable stresses on the support pillar, material plasticity data should have considered to account for the nonlinear response of the material.

4. Finite element (FE) model with results

The main reason for developing an FE model of the system was to calculate the deflections likely to occur in the glass, the deflection in the slender supports and the stresses due to the difference between the pressure within the collector and atmospheric pressure.

In the proposed design the glass is to be soldered to the enclosure base section, to model this a bonded contact was used between the glass and enclosure base section. A frictional contact with a coefficient of 0.5 was used for the contact between the glass-CPC-stainless steel slender supports. The glazing and the CPC were represented as a linear isotropic material. For the stainless-steel enclosure, base section component of the evacuated envelope, bilinear isotropic hardening material property was used to capture the material non-linearity with increasing load. The material properties considered for the components are presented in table 1,

Table 1: Material properties of components in the proposed vacuum flat plate compound parabolic concentrator collector

Component	Material	Density (Kg/m^3)	Young's modulus (E)	Poisson's ratio (ν)	UTS (MPa)
Glazing	Tempered glass	2500	70000	0.23	50
Envelope and CPC	Stainless steel	8000	193000	0.31	586

For the FEA, a quarter envelope model was considered making use of symmetry conditions to reduce the size of the computational model required as shown in figure 3.

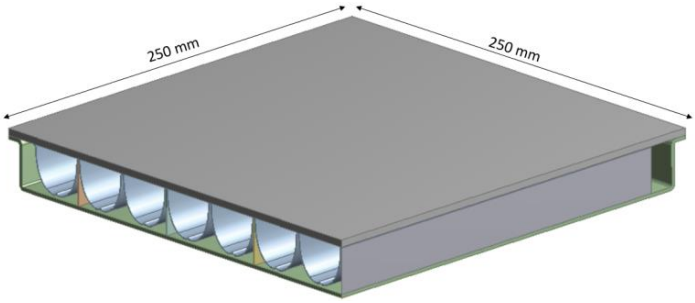

Figure 3. Quarter symmetry model of the collector geometry employed for the FEA analysis

The CPC reflector component of the system was considered to be a rigid component to minimise the required computational time, additionally, this did not influence the main area of interest which was the determination of the stresses and deformation in the glass, stainless steel back and the walls of the envelope and the supports. For the analysis, all components were meshed with shell181 elements having 4 nodes and 2 degrees of freedom per

node. Adopting a shell element model considerably reduced the computational model size and time required to solve the equations using a direct solver. The minimum orthogonal mesh quality was 0.44, the total number of elements were 46229. On the upper surface of the glass, 0.1MPa pressure was applied and the bottom surface of the enclosure base section was considered as fixed.

4.1. Predicted deformation in the glass aperture cover,

As can be seen from figure 4, the maximum predicted deformation, 0.0195mm in the glass was observed between the supports. Minimal deformation was observed towards the edges of the glass cover which were soldered to the support walls of the enclosure base section as expected.

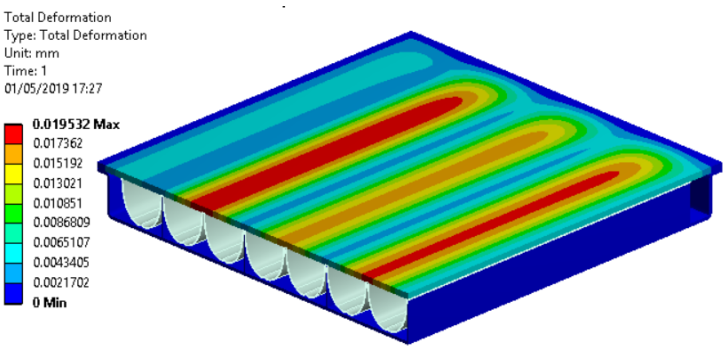

Figure 4. Total deformation of glass, mm

4.2. Predicted Equivalent Stress,

As can be seen from figure 5, a maximum equivalent stress of 11.3MPa was predicted in the glass aperture cover at the line contacts with the slender column supports. A maximum equivalent stress of 7.6MPa was predicted in the slender column supports.

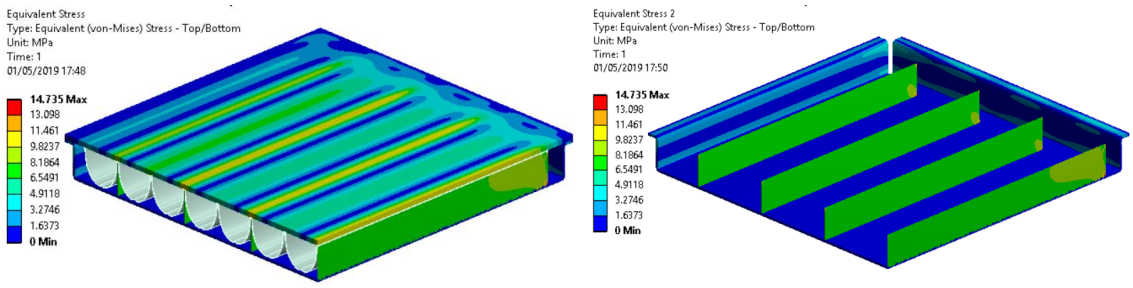

Figure 5. (a) Predicted equivalent Stress in the glass aperture cover

(b) Predicted equivalent stress in the stainless steel tray and in the slender supports, MPa

5. FE model validation

5.1 Validation of predicted glass bending and deformation,

The classical plate bending theory for thin plates developed by Kirchoff-Love is appropriate for the prediction of the deflection in the glazing because the tempered glass forming the collector aperture cover is assumed as a linear isotropic material and the expected deformation of the glass is assumed to be less than $1/10^{th}$ of the thickness (h).

According to the Kirchoff-Love theory, thin plates can be modelled by fourth order differential equations of the form presented in eq.1 [4],

$$D\Delta^2 w = D\left(\frac{\partial^4 w}{\partial x^4} + 2\frac{\partial^4 w}{\partial x^2 \partial y^2} + \frac{\partial^4 w}{\partial y^4}\right) = q \qquad \text{(eq. 1)}$$

In eq. 1, w is the displacement of the middle surface of the plate, $\Delta^{2\,in}$ eq.2 is the bi-harmonic Laplacian transform and D in eq. 3 is the flexural stiffness of the plate, q is the uniformly distributed load acting on the plate.

$$\Delta^2 = \frac{\partial^2}{\partial x^2} + \frac{\partial^2}{\partial y^2} \qquad \text{(eq. 2)}$$

$$D = \frac{Eh^3}{12(1-\nu^2)} \qquad \text{(eq. 3)}$$

The exact solution of fourth order partial differential equation defining the transverse deflection is difficult to solve unless specialised boundary conditions are assumed. Navier [4] found the solution for a rectangular plate that is simply supported on all its boundaries is given by the simplified equation,

$$w_{mn} = \frac{16p_0}{(\pi^2 mnD)\,[(m\pi/a)^2+(n\pi/b)^2]^2} \qquad \text{(eq. 4)}$$

As this equation is developed for a simply supported plate, a FE model was built for a portion of the glass envelope and enclosure where the glass can be considered to be simply supported by two adjacent slender columns and the lip of the enclosure base section. The physical dimensions of the part of the collector modelled were 66.7x450mm. The FE model was solved with a symmetry boundary condition at the center of the modelled section. The predicted maximum deflection of the glass was 0.066 mm as shown in figure 6.

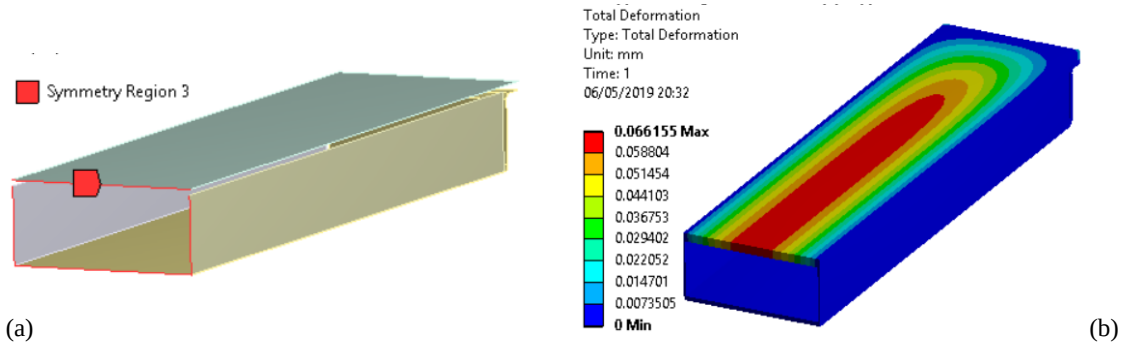

(a) (b)

Figure 6. (a) Symmetry boundary condition, (b) Predicted deflection using FEA for a section of the vacuum flat plate collector formed from the glass, stainless steel enclosure base section and two adjacent supports .

Equation 4 was solved for the known boundary conditions with the Young's Modulus E as 70000MPa, the short support length formed by the stainless steel enclosure base section (a) of 66.7mm, the long support length formed by the slender support pillar (b) of 450mm, the thickness of the tempered glass (h) as 4mm, and the Poisson's ratio (v) as 0.23, the atmospheric pressure p0 is a uniformly distributed load of 0.1MPa, m & n are Fourier series integers which are taken to be 1. Based on these values, the maximum deflection (w) was calculated to be 0.080mm. The value of deformation (0.080mm) matches the FEA predicted value (0.066mm) within 20%.

5.2 Validation of predicted stresses in slender column

In order to validate the stresses in the slender column an investigation of critical buckling load is necessary. To calculate the stresses acting on a single slender column, a section of the collector illustrated in figure. 7 is considered along with the forces acting on the glass due to the differential pressure.

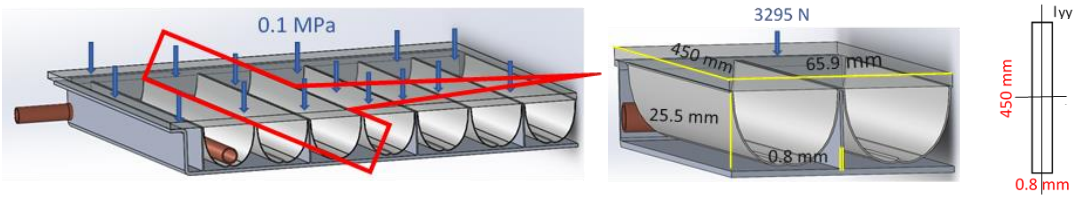

Figure 7. (a) Forces acting on the region of a single slender column support, (b) slender column support section top, (c) Cross section of slender column support.

To determine if the the slender columns will fail due to buckling, it is necessary to determine whether the column is short or long based on the slenderness ratio. Based on the literature regarding slenderness ratio if [5],

Slenderness ratio (λ) >12 – Column is long and slender and can fail under buckling phenomenon

Slenderness ratio (λ) <12 – Column is short and can fail under the crushing phenomenon

$$\lambda = \frac{l\ x\ k}{r} \qquad \text{(eq. 5)}$$

Eq. 5 provides the definition of slenderness ratio, in this case, l is the length of column as 25.5mm, k is the end connection factor and r is the minimum radius of gyration given by eq.6 ,

$$r = \sqrt{\frac{I_{min}}{A}} \qquad \text{(eq. 6)}$$

To calculate the slenderness ratio as given in eq.5, it is necessary to calculate the effective length of the column with end connection along with the minimum radius of gyration which requires calculation of the minimum moment of inertia (I_{min}).

In this case one end of the slender column, that touching the backplate of the enclosure is considered as fixed and the end touching the glazing is considered to be a pinned connection due to its potential to move against the glass surface, this requires an end connection factor (k) of 0.707[5]. So the effective length given by (l x k) is calculated to be 18.03mm.

Using the diagram of the column in figure 7(c), the moment of inertia for the section can be calculated and is presented in table 2.

Table 2: Moment of inertia in the x and y directions for the column section

	$Ixx = \frac{bh^3}{12}$	$Iyy = \frac{b^3h}{12}$
b=0.8mm, h=450mm	6075000 mm^4	19.2 mm^4

Based on the values in table 2, the minimum moment of inertia is in the y direction with I_{min} equal to 19.2mm^4 which gives the minimum radius of gyration (r) to be 0.231. Using equation 5, the slenderness ratio is calculated to be 78.066. As the slenderness ratio is greater than 12, according to the literature, regarding the definition of column slenderness ratio, the column is long and slender and it can fail due to buckling. The critical buckling load for a slender column is given by eq. 7, Euler's equation[5],

$$P_{cr} = \frac{\pi^2 E I_{yy}}{l_{eff}^2} \qquad \text{(eq. 7)}$$

Using the calculated values, the critical load for buckling to occur in the long slender column is 116.6 kN. The total load acting on the single slender column is due to the differential pressure between the enclosure pressure and atmospheric pressure and the weight of the glass.

The total load = the load acting on the cross-sectional area of a single slender column t + the weight of the glazing on the same c/s area

Substituting values the total load = (450*65.9*0.1)+(450*65.9*4*10^-9*2500) = 2965.8 N.

The density of the tempered glass used in the cover was taken to be 2500 Kg/m^3.

The stress (σ) acting on the slender column can now be determined by dividing the total load by the cross-sectional area of the slender support column,

σ = P/A = 2965.8/(450*0.8) = 8.24 MPa

Compare the above calculated stress value with the FE predicted equivalent stress result shown in figure 5(b) which is 7.6MPa, good agreement to the analytical calculation is found to within 10% accuracy.

6. Digital image correlation (DIC)

DIC is a full-field image analysis method, based on grey value digital images, that can determine the contour and displacements of objects under load. The basic operation of DIC is tracking a pattern in a sequence of images. The first image in the sequence is defined as the reference image to which the other images are compared. The reference image is considered as an undeformed image and other images as deformed. To match the reference and deformed images, DIC tracks features on the sample surface that collectively forms the speckle pattern which is artificially made on a sample surface [6].

This technique was used here to measure the deformation in the glass under vacuum pressure of 0.1Pa. A 250mmx250mm dimension collector prototype without CPC was fabricated and the glass was soldered on the top to form a vacuum-sealed, air leak-proof connection as shown in figure 8(a). Speckle pattern was created using matt white and black paint as shown in figure 8(b) to make the collector ready for DIC test.

Figure 8. (a) 250mmx250mm fabricated collector with soldered glass, (b) Speckle pattern created on prototype collector

DIC test was performed by evacuating the collector at a rate of 0.05-0.1Pa/sec from atmospheric pressure to 0.1Pa. After achieving 0.1Pa pressure the collector was held under this pressure for approximately 3 minutes. The total duration of the test was 21 minutes, over this period DIC cameras have captured a series of images at the rate of one image after every 5 seconds making 252 images in total. DIC algorithm has compared the movements within the speckle pattern of deformed images and the reference image which results are as shown in figure 9(a) and (b),

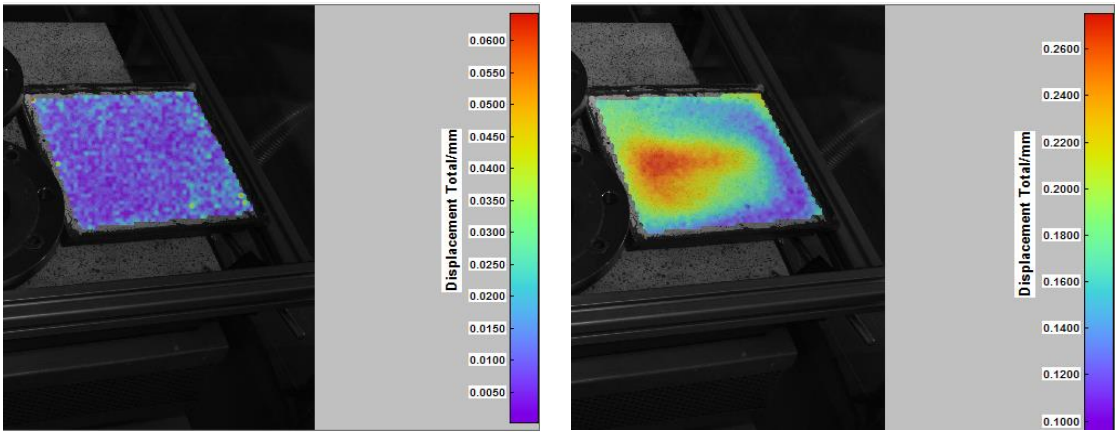

Figure 9. (a) Reference image in the first stage, (b) Total displacement in the last stage

As shown in figure 9(a), the minor displacement close to the value of 0.03mm was observed due to the vacuum pump vibrations being transferred to the collector during the experiment. As shown in figure 9(b), the maximum displacement of 0.27mm was observed in the mid-region in-between the vertical supports away from the evacuation port. In this region of maximum displacement, a point was plotted and the displacement was tracked against the number of steps as shown in figure 10.

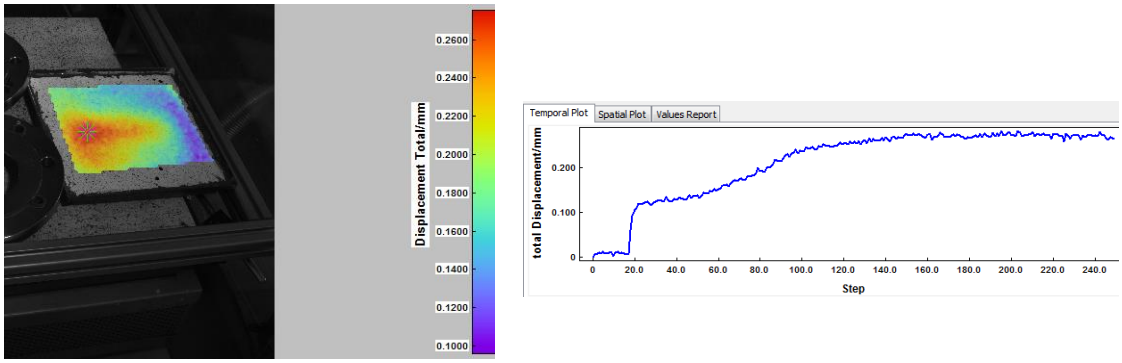

Figure 10. (a) Point plotted in high displacement region, (b) Temporal plot of displacement at a point vs the number of steps

As shown in figure 10(b), the sudden increase in the displacement at the 18th step was due to the vacuum pump start for the beginning of evacuation at atmospheric pressure. After beginning, the displacement was increasing linearly with minor deviations up to 120th step which was indicating approximate pressure of 10^2 Pa after which the displacement has stabilised until the last step till achieving 0.1Pa pressure.

It can be seen in figure 9(b) that there was a gradient on the glass surface displacement even after evacuating the collector at constant pressure and retaining the pressure for 3 minutes. It could be due to the variation in manufacturing tolerances on the fabricated metal tray of the collector. One of the slender vertical support could be slightly taller than the other or the solder joining glass to the metal could have an uneven thickness which was possibly varying the displacement unevenly on the surface.

Validation of FEA with DIC results in not possible at this stage as DIC experimentation procedure was transient and the simulation was carried out as a static analysis. But in the broader sense, we can say that the structure is able to withstand 0.1Pa vacuum pressure safely as proven by FEA and DIC experimentation results.

7. Cost Estimation

Comparative cost estimation of manufacturing an evacuated flat plate collector with an evacuated tube collector could be a vital point though it is difficult to estimate the exact cost of manufacturing processes such as low emissivity coating, CPC polishing, and glass to metal soldering at this stage of research. It can be seen from figure 2 that an envelope enclosure tray and a CPC are sheet-metal components made up of stainless steel which could be manufactured using the mechanical press in single or multiple passes. If we consider a scenario of manufacturing a 1mx1m vacuum flat plate collector, then in the case of bulk manufacturing, if the mechanical press tooling required for manufacturing is ready, then the cost of manufacturing a CPC or a tray will be approximately the cost of a single sheet of stainless steel. The table 3, below depicts approximate costs of base components with required polishing grades. Please note that these costs are based on quotations from stockists in the UK for bulk quantity order.

Table 3: Components in evacuated flat plate collector with cost per piece

Components	Cost per piece/£
SS304 2R(BA) 0.5mm standard sheet 1mx1m	40
SS304 1.2mm standard DP1 finish sheet 1mx1m	36
Tempered glass 1mx1m	23
10mm OD copper tube 10m	22.5
Total	121.5

If the cost of manufacturing processes is considered as 50% of the total cost, then the cost of manufacturing a single vacuum flat plate collector in the UK could be approximately £183 plus VAT for bulk manufacturing.

However, for an evacuated tube collector, based on the market research of the UK, the cost of 10 tubes evacuated panel having 1.5m tube length is approximately £280 plus VAT.

An important consideration in this comparison is that the purpose of vacuum flat plate collector with concentrator is to deliver working fluid at higher temperature efficiently. That means for domestic hot water and space heating purposes, smaller size panel would be sufficient compared to evacuated tube panel which could further reduce the cost of the components.

8. Conclusions

The structural integrity of a novel vacuum flat plate solar collector including CPC reflectors is assessed using FE analysis with predictions compared to analytical calculations. Values for both the predicted glass bending and stress predicted with the FE model were compared to those predicted using classical plate bending theory and Euler's buckling load calculation for slender columns.

The FEA predictions gave a maximum deflection in the glass of 0.019mm which agrees to within 20% the values determined using the analytical method predicted by considering a small rectangular section of the glass supported on slender columns and the enclosure base section. The maximum equivalent stresses predicted from the FEA analysis in the glass was 11.3MPa and in the slender column was 7.6MPa. Both values are well below the structural safety limits when compared to the ultimate tensile strength of glass (50MPa) and the yield strength of the stainless steel (230MPa). The FE stress predictions are compared to those determined using Euler's slender column buckling calculations with the stress values matching to within 10% accuracy. In addition to the stresses, the critical buckling load was calculated to be 116kN for the slender column, being considerably more than the actual load acting on the single slender column which indicates that the structural design is well within safe material property limits.

The maximum displacement in the glass and structural integrity of the collector was ensured by using DIC experimentation which proved that the collector can withstand 0.1Pa vacuum pressure safely. Finally, the approximate cost comparison showed that the cost of an evacuated flat plate collector could be less than evacuated tube collector in the case of mass manufacturing.

9. References

[1] Henshall, P., Eames, P., Arya, F., Hyde, T., Moss, R., & Shire, S. (2016). Constant temperature induced stresses in evacuated enclosures for high-performance flat plate solar thermal collectors. Solar Energy, 127, 250–261. https://doi.org/10.1016/j.solener.2016.01.025

[2] Fischer-Cripps, A. C. et al. (1995) 'Stresses and fracture probability in evacuated glazing', Building and Environment, 30(1), pp. 41–59. doi: 10.1016/0360-1323(94)E0032-M.

[3] Simko, T. M., Fischer-Cripps, A. C., & Collins, R. E. (1998). Temperature-induced stresses in vacuum glazing: Modelling and experimental validation. Solar Energy, 63(1), 1–21. https://doi.org/10.1016/S0038-092X(98)00052-8

[4] Timoshenko S.P., Woinowsky-Krieger S., 1989. Theory of Plates and Shells, secomd edition. McGraw-Hill.

[5] Timoshenko S.P., Young D.H., 1968. Elements of Strength of Materials, fifth edition. Van Nostrand.

[6] Will lepage. 2018. Digital image correlation. [Online]. [8 September 2019]. Available from: https://digitalimagecorrelation.org/